Zitierweise: *Angew. Chem. Int. Ed.* **2024**, *63*, e202406663
doi.org/10.1002/anie.202406663

Metallahelicenes

Enantiopure [6]-Azairidahelicene by Dynamic Kinetic Resolution of a Configurationally Labile [4]-Helicene

Ariadna Pazos, Carlos M. Cruz, Juan M. Cuerva, Ivan Rivilla, Fernando P. Cossío,* and Zoraida Freixa**

Abstract: A pair of enantiopure [6]-azairidahelicenes incorporating chirality at the metal center and on the helicenic ligand were synthesized by dynamic kinetic resolution (dkr) of a configurationally labile [4]-helicenic ligand (4-(2-pyridyl)-benzo[g]phenanthrene, **L1H**) using bis-cyclometalated chiral-at-metal only iridium(III) precursors as chiral inductors. The origin of the observed dkr is attributed to the different conformation and stability of diastereomeric reaction intermediates formed during the cyclometalation process. The isolated enantiomers exhibited circularly polarized phosphorescence (CPP), with $|g_{phos}|$ values of 1.8×10^{-3}.

Introduction

Organometallic helicenes are appealing chiral entities. By combining the chiroptical properties of helicenes with those inherent to the metal center, they are suitable for the development of multifunctional molecules.[1] Among them, few examples of iridahelicenes appeared in the literature, intended to exploit the outstanding photophysics of iridium(III) bis- or tris cyclometalated complexes, combined with the central chirality imposed by the organometallic core and the helicenic structure.[2] In 2010, Autschbach, Crassous, Réau, and co-workers reported the ligand 4-(2-pyridyl)-benzo[g]phenanthrene (**L1H**), and used it to construct the first examples of helicenic transition metal complexes that incorporate a metalacycle into the ortho-annulated structure of a helicene.[3] The chemistry of metalahelicenes has been thoroughly developed since then by Crassous and co-workers. That pioneering report describes the formation of the corresponding platina- and iridacyclic derivatives (**A**–**D** in Figure 1). In 2012, racemic osmium(IV) derivatives using closely related ligands were also published by Esteruelas, Sierra, and co-workers (**E** in Figure 1). It is well-established that [4]-helicenes (like **L1**-type ligands) are conformationally unstable and easily epimerize in solution.[4] Upon cyclometalation, the helicenic fragment expands, forming a conformationally robust [6]-metalahelicene. Noticeably, enantioenriched samples of compound **A** were obtained by chiral stationary phase HPLC resolution, transformed into platinum(IV) metalahelicenes (**B**), and reduced back to the original platinum(II) (**A**) whilst maintaining the helicity and enantiopurity of the metalahelicenic fragment. The metal center is also stereogenic in the case of bis-cyclometalated iridium(III) complexes (**C** and **D**). Therefore, up to 24

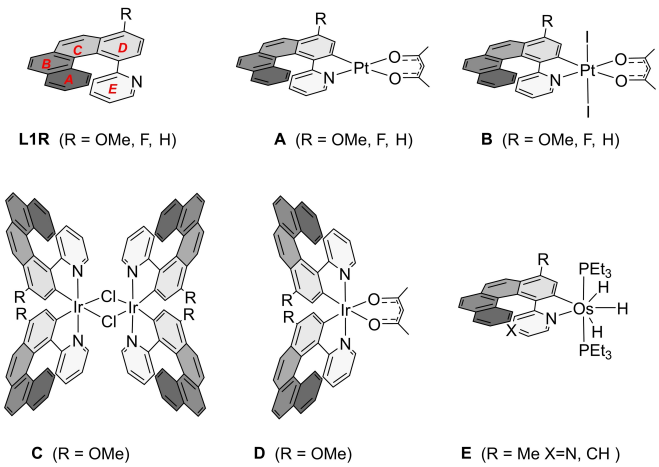

Figure 1. Organometallic compounds based on cyclometalated helicenic ligands **L1R** reported in the literature,[3,4] and ring-labeling scheme.

[*] A. Pazos, Dr. Z. Freixa
Department of Applied Chemistry, Faculty of Chemistry
University of the Basque Country (UPV/EHU)
20018, Donostia, Spain
E-mail: Zoraida_freixa@ehu.eus

Dr. C. M. Cruz, Prof. J. M. Cuerva
Department of Organic Chemistry, Unidad de Excelencia de Química (UEQ), Faculty of Sciences
University of Granada
Avda. Fuente Nueva s/n, 18071, Granada, Spain
E-mail: cmorenoc@ugr.es

Dr. I. Rivilla, Dr. Z. Freixa
IKERBASQUE, Basque Foundation for Science
48011, Bilbao, Spain

Dr. I. Rivilla, Prof. F. P. Cossío
Department of Organic Chemistry II, Faculty of Chemistry
University of the Basque Country (UPV/EHU)
20018, Donostia, Spain

Dr. I. Rivilla, Prof. F. P. Cossío
Donostia International Physics Center (DIPC)
20018, Donostia, Spain

different isomers (64 minus the meso forms) are theoretically possible for compound **C**, and up to 6 (Δ*PP*, Λ*PP*, Δ*MM*, Λ*MM*, Δ*PM*, Λ*PM*) for compound **D**. In the original publication,[3] no spectroscopic data was presented for the dimeric compound **C**. Noticeably, the molecular structure inferred from X-ray diffraction of an isolated sample revealed only one pair of enantiomers (namely, Δ*PP*Δ*PP*–**C** and Λ*MM*Λ*MM*–**C**). Compound **D** (obtained from the dimeric precursor **C** by in situ reaction with Hacac) was described as a mixture of only two enantiomeric pairs of diastereomers, isolated by column chromatography. The first eluted compound was described by the authors as "the mixture of *PM*-diastereomers", based on the ^{1}H NMR spectra in solution. The second eluted fraction, characterized by ^{1}H NMR spectroscopy and X-ray crystallography, corresponded to the mixture of Λ*PP* and Δ*MM* enantiomers. These results are rather surprising, as these core configurations were not present in the isolated X-ray structure of the precursor **C**. Therefore, either the bulk compound **C** was a more complex mixture of isomers, or the iridahelicene was not configurationally stable.

Aiming to unravel if a stereogenic bis-cyclometalated iridium(III) core would suffice to direct the helicity of **L1H** during the cyclometalation process favoring the preferential formation of certain cyclometalated diastereomers, we studied the formation of a more simple complex Ir(ppy)$_2$**L1H** (**1** in Figure 2), containing only one helicenic ligand. Compound **1** was synthesized starting from either a racemic mixture of the dimeric iridium precursor ([Ir(ppy)$_2$Cl]$_2$) or the corresponding chiral-at-metal enantiopure dimers (ΔΔ-[Ir(ppy)$_2$Cl]$_2$ and ΛΛ-[Ir(ppy)$_2$Cl]$_2$, respectively). The spectroscopic and photophysical characterization of these compounds, together with the stereochemical assignment, will be discussed here to assess the stereoselectivity of the cyclometalation process.

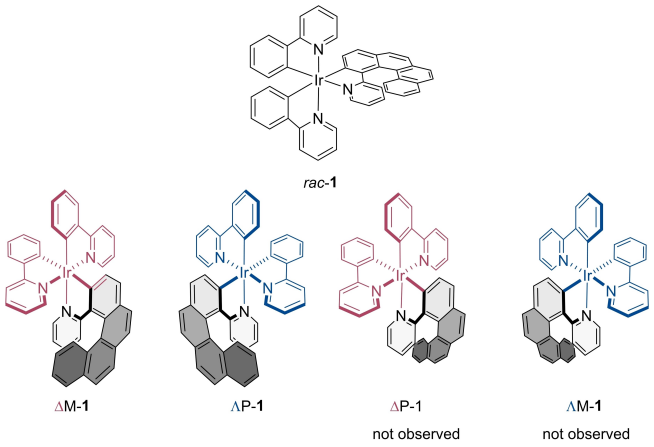

Figure 2. Compound ***rac*-1** (no stereochemistry defined) and its possible stereoisomers.

Results and Discussion

Racemic *rac*-Ir(ppy)$_2$**L1H** (***rac*-1**) was synthesized from the *rac*-[Ir(ppy)$_2$Cl]$_2$ by chloride-iridium bond cleavage in acetone through a two-step process (Scheme 1). Initially, using a chloride abstractor (AgOTf), the corresponding cationic bis-solvato [*rac*-Ir(ppy)$_2$(acetone)$_2$]$^+$ was formed. Upon separation from the formed AgCl by filtration, the bis-solvato intermediate was in situ reacted with an acetone solution containing an excess of ligand (**L1H**) and NEt_3 to favor the cyclometalation process. This is a well-established methodology for synthesizing meridional tris-cyclometalated Ir(III) compounds.[6] Up to four isomers were expected from this reaction (**Δ*P*-1**, **Λ*P*-1**, **Δ*M*-1**, and **Λ*M*-1**, Figure 2). They can be described as two enantiomeric pairs of epimers. Therefore, a statistical mixture would present two sets of 30 signals of equal intensity in the ^{1}H NMR spectra. Encouragingly, the ^{1}H NMR spectra of an aliquot of the reaction mixture at the end of the reaction (a suspension) showed only one set of 30 aromatic signals, in addition to unreacted **L1H** (Figure S6 in SI). Consistently, the solid formed at the end of the reaction, and the mother liquor revealed the same spectroscopic pattern. The coincidence of the signals in these ^{1}H NMR spectra discards a solubility-driven resolution process, and suggests a Curtin-Hammet scenario. Spin-simulation of the ^{1}H NMR spectra of a sample obtained after purification by column chromatography is consistent with the assignment to a single C_1-symmetric compound (see simulation of the spin-system in Figure 3). Additionally, this spectrum was indistinguishable from those obtained from chiral-at-metal enantiopure precursors (ΔΔ-[Ir(ppy)$_2$Cl]$_2$ and ΛΛ-[Ir(ppy)$_2$Cl]$_2$), see Figure S5). These results could be explained by either coincident ^{1}H NMR spectra for the two diastereomeric pairs of enantiomers or by actually being only one pair of enantiomers formed by

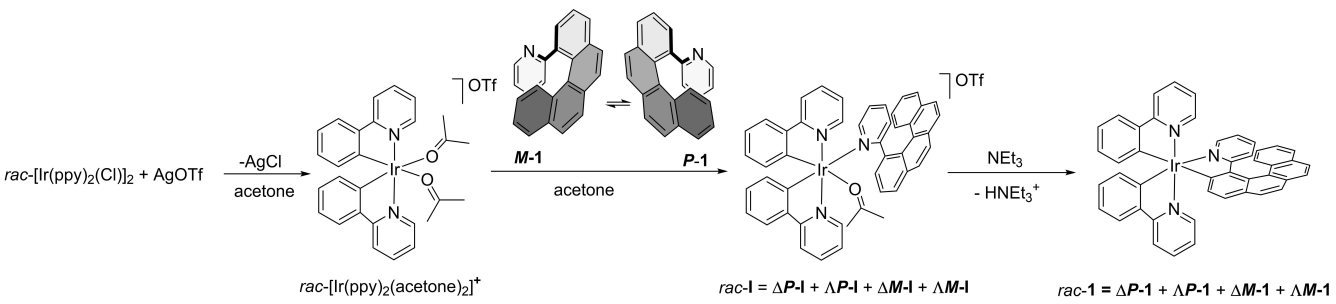

Scheme 1. Stepwise synthesis of complex ***rac*-1**, detailing the possible stereoisomers and reaction intermediates (**I**).

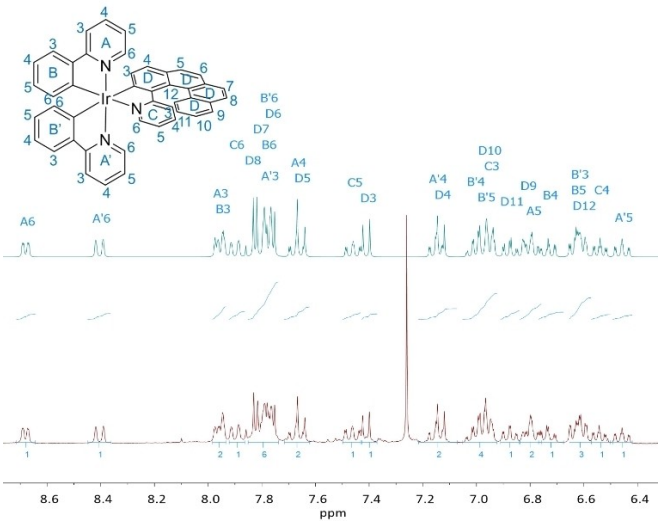

Figure 3. ^{1}H NMR spectra of compound ***rac*-1** ($CDCl_3$, 300 MHz). Experimental (bottom) and simulated with the spin system described in the Supporting Information (top). Inset shows the labeling scheme.

dynamic kinetic resolution (dkr) of the configurationally unstable [4]-helicenic ligand during cyclometalation, driven by the stereogenic metal center.[7]

The thermal stability of isolated ***rac*-1** was monitored by ^{1}H NMR in acetone-D_6 (48 h at 56 °C) and $CDCl_3$ (48 h at 61 °C), showing no signs of degradation nor epimerization (see Figures S7 and S8).

Crystals of ***rac*-1** suitable for X-ray diffraction were obtained by slow evaporation of $CDCl_3$ solutions of the compound. The molecular structure (Figure 4) confirms the formation of a [6]-azairidahelicene.[22] Accordingly, the angle between the planes containing pyridyl (E_{ring}) and metal-coordinated helicenic D_{ring} (23.00 °) is smaller than that described for the molecular structures of related free [4]-helicenic ligands (**L1OMe** and **L1Me**, Table S1). The angle between the planes containing terminal aromatic rings (A_{ring}-E_{ring}) of the metallahelicenic structure (56.91 °) is in the range of and that reported for related compounds **C** and **D.**[3,5] These structural features are reproduced in the DFT optimized geometry of **Δ*M*-1** (B3LYP/def2-TZVPP), where a E_{ring}-D_{ring} angle of 25.91 ° was found. Similarly, for the A_{ring}-E_{ring} angle, a value of 49.20 ° was obtained, which is slightly smaller than the one experimentally measured.

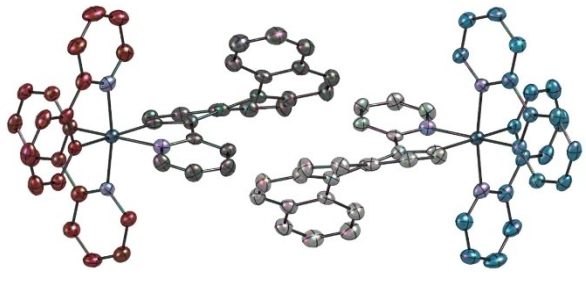

Figure 4. Molecular structure of the two enantiomers (**Λ*P*-1** and **Δ*M*-1**) present in compound ***rac*-1** according to X-ray diffraction. Ellipsoids at 50% probability. Hydrogen atoms and solvent molecules were omitted for clarity. Δ-$[Ir(ppy)_2]^+$ configuration in red, Λ-$[Ir(ppy)_2]^+$ configuration in blue, *M*-[6]-helicene in dark grey, *P*-[6]-helicene in light grey.[22]

Compound ***rac*-1** crystallized in the $P2_1/n$ centrosymmetric space group.[22] Gratifyingly, the molecular structure obtained shows that the crystal is composed exclusively by one pair of enantiomers (namely **Λ*P*-1** and **Δ*M*-1**), see Figure 4 and Figures S22, S23. The presence of only one pair of enantiomers in the crystal reinforces the hypothesis that cyclometalation occurred through metal-directed dkr of a mixture of *P*- and *M*-[4]-helicenic ligand **L1H**, which readily epimerize in solution.[8]

To further confirm this hypothesis, the electronic absorption (UV/Vis) and electronic circular dichroism (ECD) spectra of racemic and chiral-at-metal enantiopure samples of complexes ***rac*-1**, **Δ-1**, and **Λ-1** were measured. The UV/Vis spectrum of ***rac*-1** (obviously indistinguishable from those of the enantiopure derivatives, Figure S9) displays intense bands in the high-energy region (ε ~60,000 $M^{-1}cm^{-1}$), assigned to ligand-centered (^{1}LC) transitions, similar to that reported previously for other heteroleptic tris-cyclometalated iridium(III) complexes.[9] Charge transfer analysis of the time-dependent density-functional theory (TDDFT) computed transitions over the optimized structure of **Δ*M*-1** supported these observations, assigning this band to transitions with a strong intra-ligand and ligand-to-ligand charge transfer character (Figure S29), and ruled by a predominant transition at 265 nm (Table S4 and Figure S27). Additionally, there is a relatively intense band centered at ~340 nm (ε ~20,000 $M^{-1}cm^{-1}$), which could correspond to overlapping transitions with a stronger ^{1}MLCT (metal-to-ligand charge transfer) character and ligand-ligand and intraligand π→π* absorptions centered on the helicenic fragment, as predicted by TDDFT. The weaker bands in the visible part of the spectra are assigned to tailing ^{1}MLCT overlapped to spin-forbidden ^{3}MLCT transitions.

Compounds **Δ-1**, and **Λ-1** present nearly perfect mirror image ECD signals, which are rather different from those observed for enantiopure samples of the related mer-$Ir(ppy)_3$ compounds, synthesized in this work for comparative purposes (Figure 5 and Figure S19). These spectral differences point to the involvement of the orbitals of enantiopure helicene fragments in these transitions. For instance, **Λ-1** displays intense positive Cotton effects starting at ~300 nm and tailing down to 450 nm. This spectroscopic pattern is consistent with the description of ECD signals of *P*-configured carbo[6]helicenes,[10] related *P*-platina-[6]helicenes **B** and **C**,[3] and other *P*-iridahelicenes containing a Λ-configured iridium center.[2a] Noticeably, this assignment is also coherent with the configurational pairing (**Λ*P*-1** and **Δ*M*-1**) observed in the X-ray structure of compound ***rac*-1** (see above), reinforcing the hypothesis of these samples being mostly formed by one epimer (**Λ*P*-1** and **Δ*M*-1**, respectively). Additionally, a comparison of the experimental and TDDFT-simulated ECD spectra of **Δ*M*-1** underpinned the assignment (Figure S28).

The photoluminescent properties of racemic and enantiopure **1** were measured in 1×10^{-5} M CH_2Cl_2 solutions. These compounds present a phosphorescent emission band

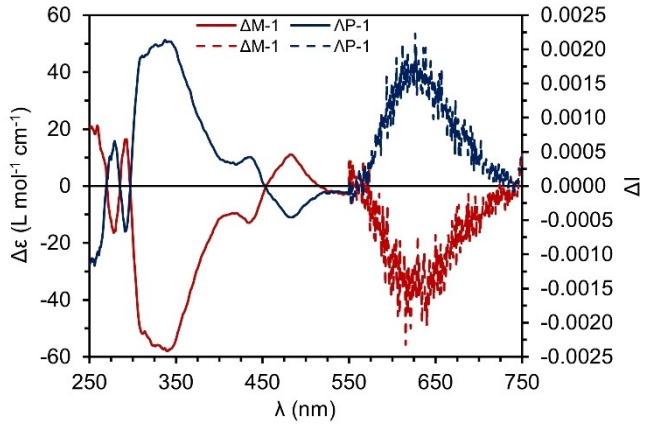

Figure 5. ECD spectra of compounds **Λ-1** (blue line) and **Δ-1** (red line), 5×10^{-5} M in CH_2Cl_2. Normalized difference of fluorescence intensity (ΔI) of compounds **Λ-1** (blue dashed line) and **Δ-1** (red dashed line) at 1×10^{-5} M in CH_2Cl_2, 283 K, $\lambda_{exc}=405$ nm.

at 656 nm ($\tau=2$ μs, $\chi^2=1.16$; $\Phi_P=4.2$ %, Figures S13–S15), which is considerably red-shifted compared to that of related *mer*-Ir(ppy)$_3$ ($\lambda=590$ nm, Figure S16). This observation is consistent with the involvement of the π* orbitals of the *ortho*-annulated aromatic ligand in the emitting ^{3}MLCT* state. The circularly polarized phosphorescence (CPP) response of **ΛP-1** and **ΔM-1** were subsequently evaluated. The measurements were conducted at 10 °C, over 1×10^{-5} M concentration solutions in deoxygenated CH_2Cl_2. Both enantiomers exhibited perfect mirrored CPP spectra, extending from 550 to 750 nm after irradiation with 405 nm LED light. Remarkably, **ΛP-1** exhibited a positive band in the CPP, while a negative one was measured on **ΔM-1**. The dissymmetry factor of the phosphorescence ($|g_{phos}|$) of both enantiomers was evaluated as 1.8×10^{-3}, similar to the obtained for cycloiridiated complexes.[2b,11] To shed light on the spin-forbidden radiative electronic transition to the ground state in **1**, we performed spin-orbit coupling TDDFT (SOC-TDDFT) calculations using the Amsterdam Density Functional (ADF) program (see Supporting Information for further details). The computed energies of the predicted SOC states, and their theoretical g_{phos} values were computed. Therefore, considering the coefficient of each triplet sublevel on phosphorescence and their g_{phos} values (see Supporting Information for further details),[12] a Boltzmann weighted $|g_{phos}|$ value of 3.1×10^{-3} was obtained, in accordance with the experimentally observed. Remarkably, the SOC-TDDFT calculations predicted the inversion of the CPP spectra with respect to the lowest energy band of the ECD spectra.

Aiming at a rational explanation for the observed dkr, an estimation of the comparative energy of diastereomeric **ΔP-1** and **ΔM-1** was evaluated using DFT calculations (see Supporting Information for details). The results show that the diastereomeric components of ***rac*-1** are nearly isoenergetic (Table S3). Noticeably, the same is not true for the putative reaction intermediates during the cyclometalation process [Ir(ppy)$_2$(**L1H**)(acetone)]$^+$ (**I** in Scheme 1),[13] being **ΔM–I** 5.48 kcal/mol more stable than **ΔP–I**. More interestingly, a visual inspection of the most stable conformers reveals that the most stable conformations of the matching combinations (**ΛP–I** and **ΔM–I**) position the activatable C–H in close proximity to the solvent-occupied site of the compound. On the contrary, in the mismatching combination (**ΔP–I** and **ΛM–I**) this group is trapped in a non-reactive quadrant of the compound, its trajectory toward the reactive site being blocked by one of the ppy ligands of the core (Figure 6 exemplifies this with the Δ-epimers). These results point to the different conformation of the reaction intermediates (**ΔP–I** and **ΛM–I** vs. **ΔM–I** and **ΛP–I**) as the most plausible explanation for the observed dkr.

In summary, all the experimental evidences (the simplicity of the ^{1}H NMR spectra of the samples of **Δ-1** and **Λ-1**, the presence of only one pair of enantiomers in the X-ray structure of ***rac*-1** and the clear signature of enantiopure helicenic fragments in the ECD and CPP spectra of **Δ-1** and **Λ-1**), point to a highly efficient dkr of the helicenic ligand during cyclometalation. These experimental results are supported by TDDFT and SOC-TDDFT calculations. Accordingly, we define these compounds as enantiopure [6]-azairidahelicenes **ΔM-1** and **ΛP-1**.

Additionally, structural and energetic comparisons of the minimum energy conformations of the reaction intermediates **Δ-I** and **Λ-I**, obtained by DFT calculations, offer a rational explanation for the observed dkr. According to these results dkr is strongly directed by structural features on the reaction intermediates towards cyclometalation, imposed by the C_2-symmetric bis-cyclometalated organometallic core. This type of arrangement is common in many organometallic compounds. Therefore, this synthetic strategy can be extended to obtain not only a variety of chiral [6]-azairidahelicenes but also other metalahelicenes by

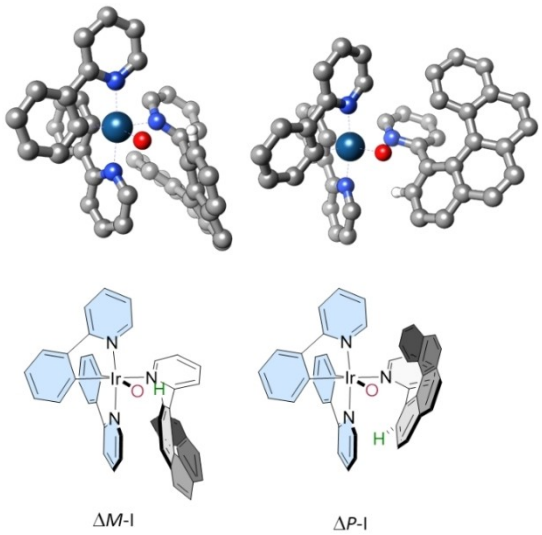

Figure 6. DFT-optimized minimum energy conformations of two epimers of the reaction intermediate Δ-[Ir(ppy)$_2$(acetone)**L1H**]$^+$ (**I**); **ΔM–I** (left) and **ΔP–I** (right),. All atoms from the coordinated acetone except oxygen have been removed for clarity. Cyclometalating C–H hydrogen is highlighted in green.

simple combinations of ready-available chiral-at-metal bischelated precursors conformationally stable and epimerizable [4]-helicene derivatives.

Supporting Information

The authors have cited additional references [13–21] within the Supporting Information.

Acknowledgements

This work was supported by projects PID2019-111281GB-I00 and PID2020-113059GB-C21 funded by MCIN/AEI/10.13039/501100011033, projects PID2022-139760NB-I00 and PID2022-137403NA-I00 funded by MCIN/AEI/10.13039/501100011033 and FEDER A way of making Europe, and IT1553-22 funded by Gobierno Vasco. The authors thank Sgiker (UPV/EHU) for technical and human support. Universidad del País Vasco (UPV/EHU, PIF20/62) (A. P.) and IKERBASQUE (Z. F. and I. R.) are acknowledged for personnel funding. C.M.C. acknowledges Junta de Andalucía for a postdoctoral grant (POSTDOC_21_00139). We thank Centro de Servicios de Informática y Redes de Comunicaciones (CSIRC), Universidad de Granada, for providing the computing time.

Conflict of Interest

The authors declare no conflict of interest.

Data Availability Statement

The data that support the findings of this study are available in the supplementary material of this article.

Keywords: Circularly Polarized Luminescence · Chiral-at-metal Complexes · Helical Structures · Iridium · Kinetic resolution

[1] a) C. Shen, E. Anger, M. Srebro, N. Vanthuyne, K. K. Deol, T. D. Jefferson, G. Muller, J. A. G. Williams, L. Toupet, C. Roussel, J. Autschbach, R. Réau, J. Crassous, *Chem. Sci.* **2014**, *5*, 1915–1927; b) N. Saleh, B. Moore Ii, M. Srebro, N. Vanthuyne, L. Toupet, J. A. G. Williams, C. Roussel, K. K. Deol, G. Muller, J. Autschbach, J. Crassous, *Chem. Eur. J.* **2015**, *21*, 1673–1681; c) M. Kos, R. Rodríguez, J. Storch, J. Sýkora, E. Caytan, M. Cordier, I. Císařová, N. Vanthuyne, J. A. G. Williams, J. Žádný, V. Církva, J. Crassous, *Inorg. Chem.* **2021**, *60*, 11838–11851; d) N. Saleh, M. Srebro, T. Reynaldo, N. Vanthuyne, L. Toupet, V. Y. Chang, G. Muller, J. A. G. Williams, C. Roussel, J. Autschbach, J. Crassous, *Chem. Commun.* **2015**, *51*, 3754–3757; e) N. Saleh, D. Kundu, N. Vanthuyne, J. Olesiak-Banska, A. Pniakowska, K. Matczyszyn, V. Y. Chang, G. Muller, J. A. G. Williams, M. Srebro-Hooper, J. Autschbach, J. Crassous, *ChemPlusChem* **2020**, *85*, 2446–2454; f) E. S. Gauthier, M. Cordier, V. Dorcet, N. Vanthuyne, L. Favereau, J. A. G. Williams, J. Crassous, *Eur. J. Org. Chem.* **2021**, *2021*, 4769–4776; g) E. S. Gauthier, L. Abella, E. Caytan, T. Roisnel, N. Vanthuyne, L. Favereau, M. Srebro-Hooper, J. A. G. Williams, J. Autschbach, J. Crassous, *Chem. Eur. J.* **2023**, *29*, e202203477; h) N. Hafedh, L. Favereau, E. Caytan, T. Roisnel, M. Jean, N. Vanthuyne, F. Aloui, J. Crassous, *Chirality* **2019**, *31*, 1005–1013; i) D. Sakamoto, I. Gay Sánchez, J. Rybáček, J. Vacek, L. Bednárová, M. Pazderková, R. Pohl, I. Císařová, I. G. Stará, I. Starý, *ACS Catal.* **2022**, *12*, 10793–10800.

[2] a) A. Macé, N. Hellou, J. Hammoud, C. Martin, E. S. Gauthier, L. Favereau, T. Roisnel, E. Caytan, G. Nasser, N. Vanthuyne, J. A. G. Williams, F. Berrée, B. Carboni, J. Crassous, *Helv. Chim. Acta* **2019**, *102*, e1900044; b) N. Hellou, M. Srebro-Hooper, L. Favereau, F. Zinna, E. Caytan, L. Toupet, V. Dorcet, M. Jean, N. Vanthuyne, J. A. G. Williams, L. Di Bari, J. Autschbach, J. Crassous, *Angew. Chem. Int. Ed.* **2017**, *56*, 8236–8239; c) J. OuYang, J. Crassous, *Coord. Chem. Rev.* **2018**, *376*, 533–547.

[3] L. Norel, M. Rudolph, N. Vanthuyne, J. A. G. Williams, C. Lescop, C. Roussel, J. Autschbach, J. Crassous, R. Réau, *Angew. Chem. Int. Ed.* **2010**, *49*, 99–102.

[4] O. Crespo, B. Eguillor, M. A. Esteruelas, I. Fernández, J. García-Raboso, M. Gómez-Gallego, M. Martín-Ortiz, M. Oliván, M. A. Sierra, *Chem. Commun.* **2012**, *48*, 5328–5330.

[5] T. Hartung, R. Machleid, M. Simon, C. Golz, M. Alcarazo, *Angew. Chem. Int. Ed.* **2020**, *59*, 5660–5664.

[6] a) M. C. DeRosa, D. J. Hodgson, G. D. Enright, B. Dawson, C. E. B. Evans, R. J. Crutchley, *J. Am. Chem. Soc.* **2004**, *126*, 7619–7626; b) J. Pérez-Miqueo, A. Telleria, M. Muñoz-Olasagasti, A. Altube, E. García-Lecina, A. de Cózar, Z. Freixa, *Dalton Trans.* **2015**, *44*, 2075–2091; c) J. Pérez-Miqueo, A. Altube, E. García-Lecina, A. Tron, N. D. McClenaghan, Z. Freixa, *Dalton Trans.* **2016**, *45*, 13726–13741.

[7] In ref [2b] a 63 : 37 diastereoselectity was reported in the cyclometalation of a [5]-helicene-NHC to a bis-cyclometalated iridium(III) core. In that case a racemic iridium dimer was reacted with a racemic sample of the conformationally robust NHC ligand containing five ortho-fused rings. Enantiomerically enriched samples of the four possible diastereomers were obtained by chiral stationary phase HPLC.

[8] N. Hellou, C. Jahier-Diallo, O. Baslé, M. Srebro-Hooper, L. Toupet, T. Roisnel, E. Caytan, C. Roussel, N. Vanthuyne, J. Autschbach, M. Mauduit, J. Crassous, *Chem. Commun.* **2016**, *52*, 9243–9246.

[9] J. C. Deaton, F. N. Castellano, in *Iridium(III) in Optoelectronic and Photonics Applications* (Ed.: E. Zysman-Colman.), John Wiley & Sons, **2017**.

[10] a) Y. Nakai, T. Mori, Y. Inoue, *J. Phys. Chem. A* **2012**, *116*, 7372–7385; b) H. Tanaka, M. Ikenosako, Y. Kato, M. Fujiki, Y. Inoue, T. Mori, *Commun. Chem.* **2018**, *1*, 38.

[11] E. S. Gauthier, N. Hellou, E. Caytan, S. Del Fré, V. Dorcet, N. Vanthuyne, L. Favereau, M. Srebro-Hooper, J. A. G. Williams, J. Crassous, *Inorg. Chem. Front.* **2021**, *8*, 3916–3925.

[12] a) J. M. Younker, K. D. Dobbs, *J. Phys. Chem. C* **2013**, *117*, 25714–25723; b) K. Mori, T. P. M. Goumans, E. van Lenthe, F. Wang, *Phys. Chem. Chem. Phys.* **2014**, *16*, 14523–14530; c) R. Inoue, R. Kondo, Y. Morisaki, *Chem. Mater.* **2022**, *34*, 7959–7970; d) H. D. Ludowieg, M. Srebro-Hooper, J. Crassous, J. Autschbach, *ChemistryOpen* **2022**, *11*, e202200020.

[13] E. C. Constable, *Polyhedron* **1984**, *3*, 1037–1057.

[14] J. G. Muntaner, L. Casarrubios, M. A. Sierra, *Org. Biomol. Chem.* **2014**, *12*, 286–297.

[15] P. K. De, D. C. Neckers, *Org. Lett.* **2012**, *14*, 78–81.

[16] a) M.-X. Song, Y. Li, D. Xu, R.-P. Deng, F.-Q. Bai, Z.-K. Qin, *RSC Adv.* **2016**, *6*, 68960–68963; b) S. Sprouse, K. A. King, P. J. Spellane, R. J. Watts, *J. Am. Chem. Soc.* **1984**, *106*, 6647–6653.

[17] O. Chepelin, J. Ujma, X. Wu, A. M. Z. Slawin, M. B. Pitak, S. J. Coles, J. Michel, A. C. Jones, P. E. Barran, P. J. Lusby, *J. Am. Chem. Soc.* **2012**, *134*, 19334–19337.
[18] F. Neese, *WIREs Comput. Mol. Sci.* **2022**, *12*, e1606.
[19] M. J. Frisch, H. B. Schlegel, G. E. Scuseria, M. A. Robb, J. R. Cheeseman, G. Scalmani, V. Barone, G. A. Petersson, H. Nakatsuji, X. Li, M. Caricato, A. Marenich, J. Bloino, B. G. Janesko, R. Gomperts, B. Mennucci, H. P. Hratchian, J. V. Ortiz, A. F. Izmaylov, J. L. Sonnenberg, D. Williams-Young, F. Ding, F. Lipparini, F. Egidi, J. Goings, B. Peng, A. Petrone, T. Henderson, D. Ranasinghe, V. G. Zakrzewski, J. Gao, N. Rega, G. Zheng, W. Liang, M. Hada, M. Ehara, K. Toyota, R. Fukuda, J. Hasegawa, M. Ishida, T. Nakajima, Y. Honda, O. Kitao, H. Nakai, T. Vreven, K. Throssell, J. A. Montgomery, Jr., J. E. Peralta, F. Ogliaro, M. Bearpark, J. J. Heyd, E. Brothers, K. N. Kudin, V. N. Staroverov, T. Keith, R. Kobayashi, J. Normand, K. Raghavachari, A. Rendell, J. C. Burant, S. S. Iyengar, J. Tomasi, M. Cossi, J. M. Millam, M. Klene, C. Adamo, R. Cammi, J. W. Ochterski, R. L. Martin, K. Morokuma, O. Farkas, J. B. Foresman, D. J. Fox, Gaussian, Inc., Wallingford CT, **2016**.
[20] a) G. te Velde, F. M. Bickelhaupt, E. J. Baerends, C. Fonseca Guerra, S. J. A. van Gisbergen, J. G. Snijders, T. Ziegler, *J. Comput. Chem.* **2001**, *22*, 931–967; b) T. Z. E. J. Baerends, A. J. Atkins, J. Autschbach, O. Baseggio, D. Bashford, A. Bérces, F. M. Bickelhaupt, C. Bo, P. M. Boerrigter, C. Cappelli, L. Cavallo, C. Daul, D. P. Chong, D. V. Chulhai, L. Deng, R. M. Dickson, J. M. Dieterich, F. Egidi, D. E. Ellis, M. van Faassen, L. Fan, T. H. Fischer, A. Förster, C. Fonseca Guerra, M. Franchini, A. Ghysels, A. Giammona, S. J. A. van Gisbergen, A. Goez, A. W. Götz, J. A. Groeneveld, O. V. Gritsenko, M. Grüning, S. Gusarov, F. E. Harris, P. van den Hoek, Z. Hu, C. R. Jacob, H. Jacobsen, L. Jensen, L. Joubert, J. W. Kaminski, G. van Kessel, C. König, F. Kootstra, A. Kovalenko, M. V. Krykunov, P. Lafiosca, E. van Lenthe, D. A. McCormack, M. Medves, A. Michalak, M. Mitoraj, S. M. Morton, J. Neugebauer, V. P. Nicu, L. Noodleman, V. P. Osinga, S. Patchkovskii, M. Pavanello, C. A. Peeples, P. H. T. Philipsen, D. Post, C. C. Pye, H. Ramanantoanina, P. Ramos, W. Ravenek, M. Reimann, J. I. Rodríguez, P. Ros, R. Rüger, P. R. T. Schipper, D. Schlüns, H. van Schoot, G. Schreckenbach, J. S. Seldenthuis, M. Seth, J. G. Snijders, M. Solà, M. Stener, M. Swart, D. Swerhone, V. Tognetti, G. te Velde, P. Vernooijs, L. Versluis, L. Visscher, O. Visser, F. Wang, T. A. Wesolowski, E. M. van Wezenbeek, G. Wiesenekker, S. K. Wolff, T. K. Woo, A. L. Yakovlev, SCM, Theoretical Chemistry, Vrije Universiteit, Amsterdam, The Netherlands, **2023**.
[21] F. Plasser, *J. Chem. Phys.* **2020**, *152*, 084108.
[22] Deposition Number 2350083 (for ***rac*-1**) contains the supplementary crystallographic data for this paper. These data are provided free of charge by the joint Cambridge Crystallographic Data Centre and Fachinformationszentrum Karlsruhe Access Structures service.

Manuscript received: April 8, 2024
Accepted manuscript online: April 24, 2024
Version of record online: May 24, 2024